Surgical and Radiologic Anatomy (2020) 42:219–228
https://doi.org/10.1007/s00276-019-02308-6

ORIGINAL ARTICLE

Frequency, location, and morphology of accessory maxillary sinus ostia: a retrospective study using cone beam computed tomography (CBCT)

Kuofeng Hung[1] · Carla Montalvao[1] · Andy Wai Kan Yeung[1] · Gang Li[2] · Michael M. Bornstein[1]

Received: 29 April 2019 / Accepted: 20 August 2019 / Published online: 27 August 2019

Abstract

Purpose To evaluate the reliability of cone beam computed tomography (CBCT) imagining in the assessment of the frequency, location, and morphological characteristics of accessory maxillary ostia (AMOs), and to analyze a potential association with sinus and dentoalveolar pathologies.

Methods CBCT scans with bilateral maxillary sinuses that were acquired from September 2016 to September 2018 were initially screened. A total of 160 CBCT scans (320 sinuses) that fulfilled the inclusion criteria were included for further analysis. The presence, location, and morphological characteristics of the AMOs were evaluated in axial, coronal, and sagittal CBCT views. The findings were correlated with age, gender, sinus, and dentoalveolar pathology to assess for potential influencing factors on AMOs.

Results An AMO was present in 151 (47.2%) of the 320 sinuses. Most of the AMOs were located within the region of the nasal fontanelle or hiatus semilunaris (81.1%) presenting with an ovaloid (48.4%) or a round shape (39.0%). The average length of the AMOs was 2.33 ± 1.42 mm, occupying an area of 3.43 ± 4.51 mm^2, respectively. Morphological changes of the maxillary sinus mucosa were positively associated with length and area of AMOs. Furthermore, the status of the dentition in the posterior maxilla seemed to be an influencing factor on AMO shape.

Conclusions Nearly half of the maxillary sinuses assessed in the present study population had an AMO. Pathologies of the maxillary sinus seem to have an impact on AMOs, which is demonstrated here by morphological changes of the sinus mucosa being associated with an increase in length and area of accessory ostia.

Keywords Maxillary sinus · Accessory maxillary ostia · Cone beam computed tomography · Frequency

Introduction

The maxillary sinus is the largest paranasal sinus, and of great interest to otorhinolaryngology and dental medicine alike. The diagnosis of health versus pathology of the maxillary sinuses is important prior to functional endoscopic sinus surgeries [9], and sinus-related dental surgeries, such as maxillary sinus floor elevation procedures [3]. These surgical interventions may influence the physiological condition of the sinus, and possibly increase the risk for post-operative complications including sinusitis [9, 29]. To reduce the risk of such complications, a thorough radiological assessment of the maxillary sinus is imperative prior to surgical interventions in the sinus region [4, 9].

The primary maxillary ostium (PMO) is a natural opening located on the junction of the medial wall of the maxillary sinus and the floor of the orbit [20]. Its patency contributes to an adequate drainage from the sinus into the hiatus semilunaris, the middle meatus, and then the nasal cavity. The PMO, therefore, helps to maintain a physiological and healthy condition of the maxillary sinus [26].

The accessory maxillary ostium (AMO) is regarded as any extra opening other than the PMO, and is usually present in the region of the nasal fontanelle (NF) or hiatus semilunaris (HS) [13, 23]. The NF is to be found in the middle

✉ Michael M. Bornstein
bornst@hku.hk

[1] Oral and Maxillofacial Radiology, Applied Oral Sciences and Community Dental Care, Faculty of Dentistry, The University of Hong Kong, Hong Kong SAR, China

[2] Department of Oral and Maxillofacial Radiology, Peking University School and Hospital of Stomatology, Beijing, China

meatus located below the uncinate process and above the inferior turbinate, covered by the nasal mucous membrane medially, the mucosa of the maxillary sinus laterally, and a layer of connective tissue in between [15]. The presence of an AMO enables to not only increase the ventilation rate of the maxillary sinus [11], but also leads to an inverse drainage from the middle meatus into the sinus [28]. This results in a reduced nitric oxide concentration and mucus accumulation in the sinus, which possibly contributes to pathological changes, such as mucosal thickening, mucous retention cyst formation, and maxillary sinusitis [28]. Some cadaveric and endoscopic studies reported that the AMO is a round or an oval opening with a wide range in size varying from 0.5 to 10 mm [13, 23, 28], and has a frequency ranging from 0 to 43% [15]. However, the evaluation of the characteristics of the AMO in cadavers is challenging due to the deformation of anatomical structures following dissection.

Cone beam computed tomography (CBCT) has been recommended for the visualization of anatomical structures and to identify anatomical variations or pathological changes in the maxillofacial region, particularly in the maxillary sinus [5, 14]. There are some CT/CBCT studies that have reported on the frequency of AMOs [1, 6, 7, 18, 28, 29], and the association between AMO presence and sinus pathologies [1, 6, 8, 28, 29]. However, it remains unknown whether the presence, location, and morphological characteristics (shape and dimension) of AMOs have a potential association with gender, age, changes of the sinus mucosa, and dentoalveolar pathology. Therefore, the purpose of this study was to evaluate the reliability of CBCT imagining in the assessment of the frequency, location, and morphological characteristics of AMOs. Additionally, a potential association of influencing factors including gender, age, changes of the sinus mucosa, and dentoalveolar pathology with AMO characteristics was evaluated to provide more information and knowledge, which could be valuable for the assessment of maxillary sinuses prior to sinus-related surgeries.

Materials and methods

Study population

In the present retrospective study, 205 CBCT scans with a medium to large field of view (FOV) that depicted bilateral maxillary sinuses were initially eligible for evaluation. These scans had been performed from September 2016 to September 2018 using a ProMax 3D Mid (Planmeca, Helsinki, Finland) in patients referred to the Diagnostic Imaging Clinic at the Prince Philip Dental Hospital, which also houses the Faculty of Dentistry of the University of Hong Kong. After screening of the scans, 45 CBCTs were excluded based on the following exclusion criteria:

1. Patients < 18 years old ($n = 5$ scans excluded).
2. Bilateral maxillary sinuses not entirely visible on the CBCT scan ($n = 7$).
3. Patients having experienced surgeries or with a history of trauma in the region of the maxillary sinus ($n = 28$, including 17 due to orthognathic surgery, 9 due to sinus floor elevation, 1 due to sinus fracture, and 1 due to planning of surgery due to osteoradionecrosis).
4. Artifacts (acquisition or patient-related) presenting in the maxillary sinus region ($n = 3$).
5. Pathology from anterior teeth (canine-to-canine) impinging into the maxillary sinuses ($n = 2$).

Therefore, a total of 160 CBCT scans (320 sinuses) were included for further analysis in the present study.

The study was conducted in full accordance with the Declaration of Helsinki 2013 (www.wma.net). The study protocol was submitted to and approved by the local institutional review board of the University of Hong Kong/Hospital Authority Hong Kong West Cluster (approval number UW 18-499), and registered in the HKU Clinical Trials Registry (study identifier HKUCTR-2531).

CBCT image analysis of primary (PMO) and accessory maxillary ostia (AMO)

CBCT images were assessed on a Philips 223 V LED monitor with a resolution of 1920 × 1080 pixels (Philips, Amsterdam, The Netherlands). Data were reconstructed with slices of 0.5 mm thickness and a 0.4 mm voxel size. All images were evaluated using the same software (ROMEXIS Version 4.4.0.R, Planmeca, Helsinki, Finland). Two examiners (KH and CM) performed all observations to test for inter-observer reproducibility, and one examiner (KH) performed all observations twice with a time gap of a minimum of 1 month between each observation to test for intra-observer repeatability. Inconsistent findings were resolved by discussion to reach a final diagnosis that was used for further reporting and statistical analyses.

In the included CBCT scans, the bilateral maxillary sinuses were both assessed. First, the presence of the primary ostium was recorded as:

1. Radiologically absent.
2. Radiologically present.

Afterward, the sinuses were evaluated for the presence (radiologically absent/present) and number of AMOs. Sinuses with AMOs were categorized into two groups for further analysis:

1. Sinus with single AMO.
2. Sinus with multiple AMOs.

If present, the location of the AMO was judged in coronal CBCT views by its position on the medial wall of the maxillary sinus, and was evaluated as follows:

1. *AMO located within the region of NF/HS* AMO located in the region of the uncinate process, or located in the region between the attachments of the inferior turbinate and middle turbinate.
2. *AMO located outside the region of NF and HS* AMO located in the region between the attachment of the inferior turbinate and the most caudal point of the medial wall of the maxillary sinus, or in the region between the attachment of the middle turbinate and the most cranial point of the medial wall of the maxillary sinus.

Additionally, the shape of the AMO was assessed in the adjusted sagittal CBCT view as:

1. Round.
2. Ovaloid.
3. Slit shaped.

According to the shape, the following dimensions of the AMO were measured (in mm) in the adjusted sagittal CBCT view:

1. L_A The length of the long axis (round/ovaloid)/the length of the AMO (slit shaped).
2. S_A The length of the short axis (round/ovaloid)/the width of the AMO (slit shaped).

Based on the lengths measured, the further parameters were calculated as follows:

1. L/S ratio $=\frac{L_A}{S_A}$.
2. AMO area $(mm^2)=\frac{\pi L_A S_A}{4}$ (round/ovaloid)/$L_A \times S_A$ (slit shaped).

CBCT image analysis of maxillary sinus health and status of the dentition

The status of the maxillary sinus and the dentition was recorded to assess a potential association with AMO presence and number. For the Schneiderian membrane and its bony lining, the status was recorded according to an adapted classification from Soikkonen and Ainamo as used in the previous studies [24, 29]:

1. Inconspicuous or up to 2 mm thickening of the sinus membrane.
2. Flat, shallow thickening of the Schneiderian membrane (> 2 mm).
3. Semispherical thickening of the membrane (suspected mucous retention cyst).
4. Complete opacification of the sinus.
5. Mixed flat and semispherical thickenings.
6. Other (e.g., bone destruction, cyst, foreign body, suspected neoplasia).

For further data analysis, the status of the maxillary sinus was categorized into healthy (1) or pathological (2–6).

For all CBCT scans included, the status of the dentition distal to the maxillary canine, with inclusion of the third molar, was classified into:

1. Dentate.
2. Partially edentulous.
3. Completely edentulous.

For further data analysis, the status of the dentition of the posterior maxilla was categorized into dentate (1) or (partially) edentulous (2, 3).

If teeth were present in the posterior maxilla, their statuses were evaluated to account for potential endodontic or periodontal pathology that could influence the status of the maxillary sinus. The endodontic status of teeth in the respective posterior maxilla was classified into (assigning the largest code value whenever applicable):

1. No endodontic pathology or treatment.
2. Endodontic treatment(s) without visible pathology.
3. Apical lesion(s) with or without visible endodontic treatment(s).

Similarly, teeth with periodontal pathology were classified into (assigning the largest code value whenever applicable):

1. No periodontal lesions.
2. Horizontal and/or vertical periodontal bone lesions deeper than the midlevel of the respective root without furcation involvement.
3. Periodontal bone lesions with furcation involvement.

For further data analysis, the endodontic/periodontal status was categorized into healthy (1) or pathological (2, 3).

Statistical analysis

All data listed were first analyzed descriptively. Cohen kappa values and intra-class correlation coefficients were calculated for intra-observer repeatability and inter-observer reproducibility. The assessments of potential influencing factors on AMO presence and number were done on a patient level (age and gender) and a sinus level (morphological

changes of the sinus mucosa, status of the dentition, endodontic and periodontal pathology), respectively. Potential influencing factors on AMO presence and number were evaluated with either Chi-square test or Mann–Whitney *U* test. To account for the possible patient clustering effect, the significance of potential influencing factors on the characteristics of AMOs were evaluated on an AMO level with generalized estimating equations models with identity link function (continuous responses) or logistic regression (binary responses) [16].

The significance level chosen for all statistical tests was $p < 0.05$. All analyses were performed in SPSS (Version 25.0, IBM Corp., Armonk, New York, USA).

Results

In the present study, 320 sinuses from a total of 160 CBCT scans were analyzed. The included CBCT scans were from 99 female and 61 male patients with a mean age of 33.3 years (ranging from 19 to 84 years). The FOV of the included scans was 20 × 17 cm for 125 patients, 20 × 10 cm for 24 patients, and 10 × 10 cm for 11 patients.

A PMO was radiologically present in 313 (97.8%) of the 320 assessed sinuses (Table 1, Fig. 1). For the remaining seven sinuses, a PMO could not be detected as the ethmoidal infundibulum region was covered by a thickened mucosa. Therefore, the PMO was categorized as radiologically absent for these sinuses. Nearly half of the sinuses assessed were considered to be healthy or with a shallow Schneiderian membrane thickening of < 2 mm (49.7%), and the majority of these sinuses were associated with a dentate dentition (64.1%) with no endodontic pathology or treatment (85.7%) and no periodontal bone loss (83.5%; Table 1). The most frequent morphological change of the Schneiderian membrane was flat shallow thickening > 2 mm (27.8%).

Intra- and inter-observer agreement

Intra-observer repeatability was excellent regarding the presence, location, shape, and dimensions of the AMOs, and morphological changes of sinus mucosa, status of the dentition, endodontic and periodontal status (Table 2). Inter-observer reproducibility was excellent regarding the location of the AMOs and status of the dentition. The reproducibility regarding the presence, shape, and

Table 1 Demographic data including gender, age (patient level), and morphological changes of the Schneiderian membrane, status of the dentition, endodontic and periodontal statuses (sinus level)

	Male	Female	All (160 patients)
Gender	61 (38.1%)	99 (61.9%)	160 (100%)
Age (mean)	32.9	33.6	33.3
	Male	Female	All (320 sinuses)
Morphological changes of sinus mucosa			
Healthy/shallow thickening of < 2 mm	51 (41.8%)	108 (54.6%)	159 (49.7%)
Flat shallow thickening of > 2 mm	41 (33.6%)	48 (24.2%)	89 (27.8%)
Semispherical mucosal thickening	17 (14.0%)	22 (11.1%)	39 (12.2%)
Complete opacification of sinus	1 (0.8%)	2 (1.0%)	3 (0.9%)
Mixed flat/semispherical thickening	11 (9.0%)	13 (6.6%)	24 (7.5%)
Other	1 (0.8%)	5 (2.5%)	6 (1.9%)
Status of the dentition in the posterior maxilla			
Dentate	86 (70.5%)	119 (60.1%)	205 (64.1%)
Partially edentulous	33 (27.0%)	70 (35.4%)	103 (32.2%)
Completely edentulous	3 (2.5%)	9 (4.5%)	12 (3.7%)
Endodontic status (first premolar to third molar)			
No endodontic pathology or treatment	102 (85.7%)	162 (85.7%)	264 (85.7%)
Endodontic treatment(s) without visible pathology	4 (3.4%)	12 (6.4%)	16 (5.2%)
Apical lesion(s) with/without endodontic treatment(s)	13 (10.9%)	15 (7.9%)	28 (9.1%)
Periodontal status (first premolar to third molar)			
No periodontal lesions	95 (79.8%)	162 (85.7%)	257 (83.5%)
Periodontal bone loss without furcation involvement	16 (13.5%)	14 (7.4%)	30 (9.7%)
Periodontal bone loss with furcation involvement	8 (6.7%)	13 (6.9%)	21 (6.8%)
PMO presence	120 (98.4%)	193 (97.5%)	313 (97.8%)

PMO, primary maxillary ostium

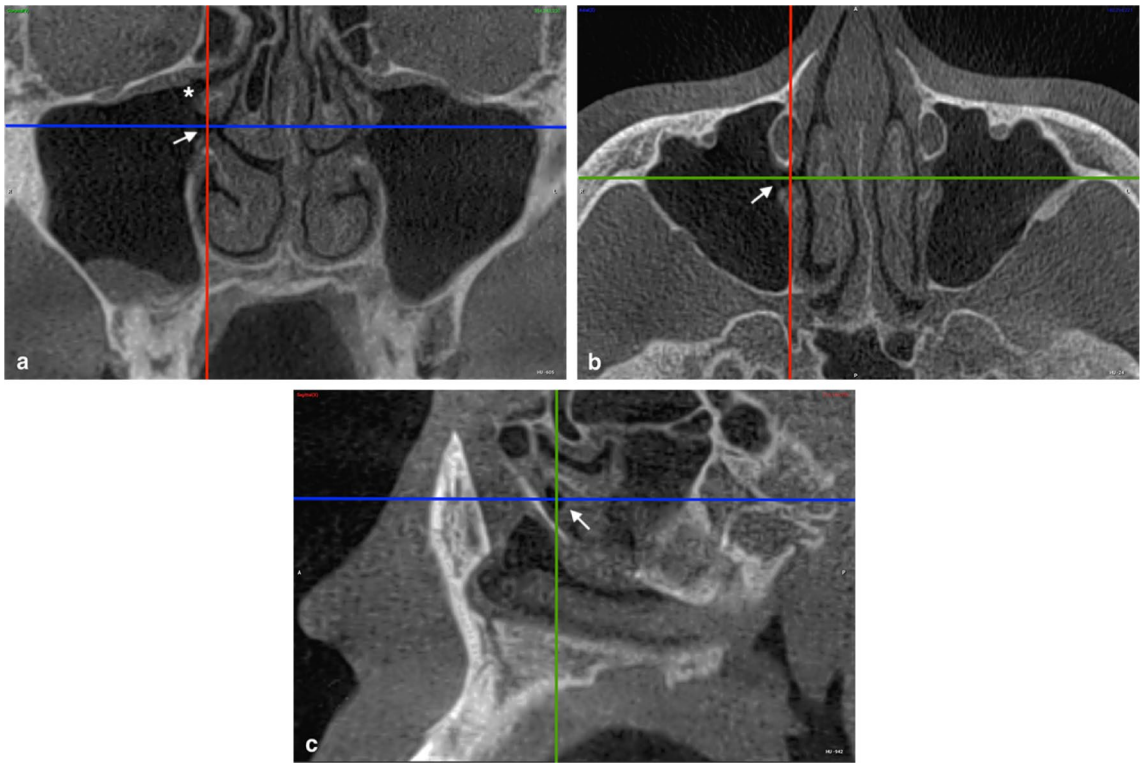

Fig. 1 Representative CBCT image illustrating a PMO (asterisk) and an AMO (white arrow) present in the same patient (**a** coronal view; **b** axial view; **c** sagittal view)

Table 2 Analysis of intra- and inter-observer agreement

Observed parameters	Intra-observer	Inter-observer
AMO		
Presence	0.86	0.67
Number	0.73	0.58
Location	0.93	0.86
Shape	0.80	0.63
Length of the long axis	0.92[a]	0.69[a]
Length of the short axis	0.84[a]	0.64[a]
Morphological changes of sinus mucosa	0.83	0.73
Status of the dentition in the posterior maxilla	0.93	0.90
Endodontic status	0.81	0.62
Periodontal status	0.82	0.68

Cohen kappa value was calculated unless otherwise mentioned

Agreement was rated as "low" (< 0.41), "moderate" (0.41–0.60), "substantial" (0.61–0.80), and "excellent" (> 0.80)

AMO accessory maxillary ostium

[a]Intra-class correlation coefficients

dimensions of the AMOs, and morphological changes of sinus mucosa, endodontic and periodontal pathology exhibited a substantial agreement (Table 2).

Table 3 Descriptive analysis of AMO presence, number, location, shape, and dimensions

	Male	Female	Total
Presence			
Present	57 (46.7%)	94 (47.5%)	151 (47.2%)
Absent	65 (53.3%)	104 (52.5%)	169 (52.8%)
Total	122 (100%)	198 (100%)	320 (100%)
Number			
One	45 (79.0%)	74 (78.7%)	119 (78.8%)
Two	8 (14.0%)	17 (18.1%)	25 (16.6%)
Three	4 (7.0%)	3 (3.2%)	7 (4.6%)
Total	57 (100%)	94 (100%)	151 (100%)
Location			
Within NF/HS	59 (80.8%)	95 (81.2%)	154 (81.1%)
Outside NF/HS	14 (19.2%)	22 (18.8%)	36 (18.9%)
Total	73 (100%)	117 (100%)	190 (100%)
Shape			
Round	28 (38.4%)	46 (39.3%)	74 (39.0%)
Ovaloid	40 (54.8%)	52 (44.5%)	92 (48.4%)
Slit shaped	5 (6.8%)	19 (16.2%)	24 (12.6%)
Total	73 (100%)	117 (100%)	190 (100%)
Dimensions			
Length of the long axis (mm)			
Mean ± SD	2.34 ± 1.42	2.32 ± 1.43	2.33 ± 1.42
Median (IQR)	2.04 (1.67)	2.00 (1.61)	2.00 (1.62)
Length of the short axis (mm)			
Mean ± SD	1.52 ± 0.86	1.40 ± 0.76	1.45 ± 0.80
Median (IQR)	1.20 (1.19)	1.20 (0.95)	1.20 (0.95)
L/*S* ratio			
Mean ± SD	1.57 ± 0.52	1.76 ± 0.86	1.68 ± 0.75
Median (IQR)	1.49 (0.79)	1.56 (1.00)	1.50 (0.89)
AMO area (mm^2)			
Mean ± SD	3.63 ± 4.70	3.31 ± 4.40	3.43 ± 4.51
Median (IQR)	2.03 (4.01)	1.66 (3.52)	1.92 (3.64)

AMO accessory maxillary ostium, *HS*, hiatus semilunaris, *NF* nasal fontanelle, *SD* standard deviation, *IQR*, interquartile range

Characteristics of AMOs

An AMO was radiologically present in 151 (47.2%) of the 320 sinuses assessed (Table 3). In the 151 sinuses diagnosed with AMOs, 32 sinuses (21.2%) had more than 1 AMO (Table 3). Altogether, 190 AMOs were found in the 151 sinuses and most AMOs were located within the region of NF/HS (81.1%) (Table 3, Fig. 2). The majority of the AMOs were of an ovaloid (48.4%) followed by a round shape (39.0%) (Table 3, Fig. 3). The average lengths of long and short axes of the AMOs were 2.33 ± 1.42 mm (median 2 mm) and 1.45 ± 0.80 mm (median 1.2 mm), respectively (Table 3). The average *L*/*S* ratio and AMO area were 1.68 ± 0.75 (median 1.50) and 3.43 ± 4.51 mm^2 (median 1.92 mm^2), respectively (Table 3).

Potential influencing factors on the characteristics of AMOs

The analysis of the 320 sinuses from 160 CBCT images exhibited that age, gender, morphological changes of the sinus mucosa, status of the dentition, and periodontal pathology did not have a significant effect on the presence of an AMO (Table 4). However, significantly more sinuses associated with no endodontic pathology were diagnosed with an AMO (49.6% versus 31.8%; $p = 0.028$). All potential influencing factors did not have a significant effect on AMO number (single/multiple) (Table 4).

Regarding the characteristics of the AMOs, a multilevel modeling analysis was performed on the 190 AMOs observed in 151 sinuses out of the 320. The status of the dentition in the posterior maxilla exhibited a significant association with AMO shape (Table 5). Partial/complete edentulism was associated with a higher chance of having a round shape (OR = 2.85, $p = 0.002$), while a dentate dentition was associated with an ovaloid AMO shape (OR = 0.46, $p = 0.022$) (Table 5). Further, partial/complete edentulism was associated with a smaller *L*/*S* ratio (OR = 0.75, $p = 0.010$) compared to dentate patients (Table 5). The morphological changes of sinus mucosa were positively associated with the length of the AMO long axis (OR = 1.75, $p = 0.013$) and AMO area (OR = 5.92, $p = 0.020$) (Table 5). The periodontal status exhibited a negative association with the length of the AMO long axis (OR = 0.56, $p = 0.007$) and AMO area (OR = 0.18, $p = 0.004$) (Table 5).

Discussion

The present study assessed the frequency, location, and morphological characteristics of AMOs in 320 maxillary sinuses from 160 CBCT images, and investigated whether age, gender, changes of the sinus mucosa, status of the dentition, endodontic and periodontal pathology may be potential influencing factors. Results showed that the frequency of AMOs in the sinuses assessed is 47.2% (151/320), which is above the range reported by previous cadaveric (0–43%, median 23%) [15], endoscopic (9–23%, median 19.3%) [2, 8, 12, 15, 17, 19, 22], CT (19.1 and 37.1%) [18, 28], and CBCT (23.7–45.5%, median 40.1%) [1, 6, 7, 29] studies. The differences reported are clearly less pronounced for investigations using CBCT imaging, which may result from the high spatial resolution of this technique that increases the accuracy of identifying small anatomical variations in the maxillary sinus [27].

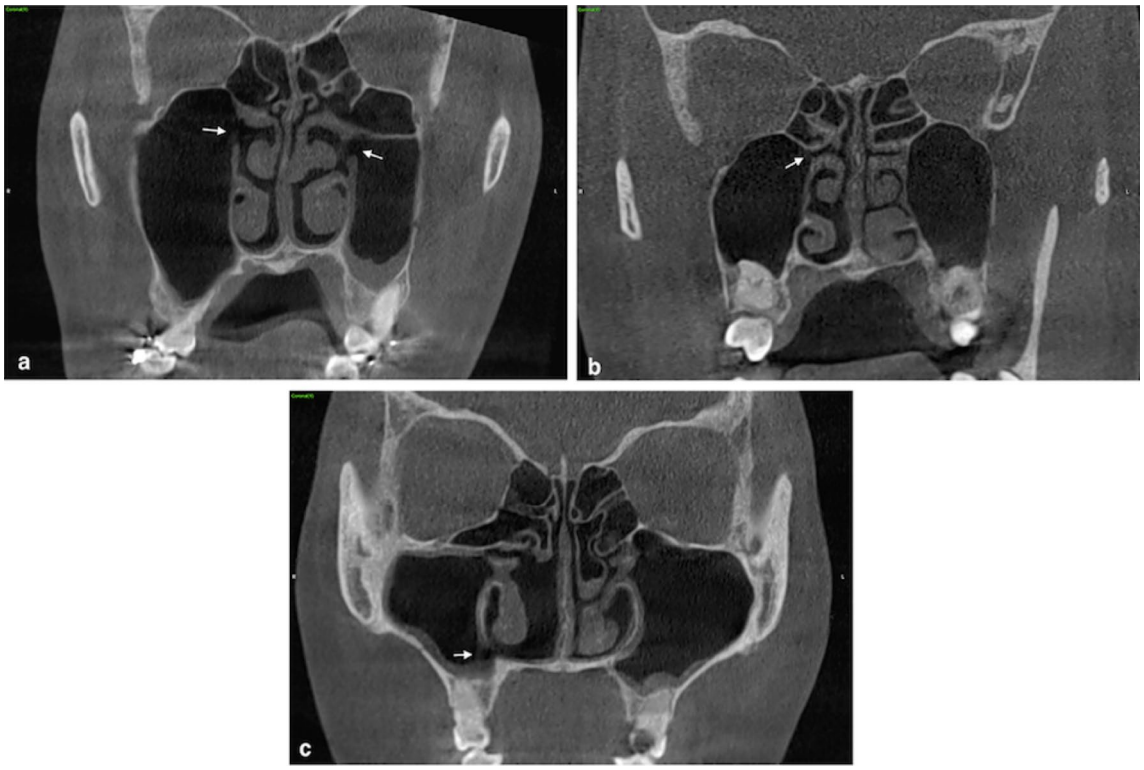

Fig. 2 Representative CBCT images (coronal views) illustrating various AMOs (white arrow) located within the region of the nasal fontanelle (**a**) and outside the region of the nasal fontanelle (**b**, **c**)

It is of great importance to differentiate the PMO from AMOs in CBCT images. The PMO is characterized by the fact that it is located on the cranial part of the medial wall of the maxillary sinus and opens into the narrow ethmoidal infundibulum along with the uncinate process [10, 25, 29]. In the present analysis, 313 (97.8%) of the 320 sinuses observed had a clearly visible PMO. Due to mucosal thickening at the ethmoidal infundibulum region, the PMO was not radiologically present in the remaining seven sinuses, of which two were observed with the presence of an AMO.

An AMO is generally considered to be located in the region of the NF or HS, and connecting the sinus to the middle meatus of the nasal cavity. However, there is still a dispute about the exact location of AMOs. Rice and Schaeffer [21] termed all extra openings of the maxillary sinus other than a single PMO as AMOs, irrespective of their location. In the present study, 36 (18.9%) of the 190 AMOs detected were located outside the region of NF and HS, and connected the respective sinuses to the inferior or superior meatus. This finding may explain the slightly higher frequency of AMOs reported here in comparison with the previous studies that focused on the region of NF and HS only.

The clearance of the sinus secretion from the maxillary sinus through the PMO into the middle meatus of the nasal cavity normally depends on the mucociliary action of its lining mucosa. The presence of an AMO has been reported to cause re-entry of sinus secretions drained through the PMO into the maxillary sinus, which may influence the condition of the sinus [28]. Some studies suggested a thorough radiological assessment for the presence of an AMO prior to surgical interventions in the sinus region including functional endoscopic sinus surgeries, maxillary sinus floor elevation procedures, apical surgery, and the removal of impacted teeth in the posterior maxilla [1, 7, 8, 12, 28, 29]. However, it is still disputed whether the presence of AMOs has a direct association with morphological changes of the sinus mucosa [1, 6, 8, 12, 29]. In the present study, the analysis on the 320 sinuses exhibited that the presence of an AMO was not associated with the morphological changes of the sinus mucosa, which is in line with the two previous CBCT studies [6, 29]. Nevertheless, the subsequent multilevel modeling analysis on the characteristics of the 190 AMOs detected in 151 sinuses exhibited that having morphological changes of the sinus mucosa was a factor associated with an increase in AMO area. Based on these findings, together with a positively skewed distribution of the data regarding the AMO area (mean 3.43 mm^2 and median 1.92 mm^2), it might be speculated that morphological changes of the sinus mucosa are more related to the size of an AMO than its presence. This hypothesis might also

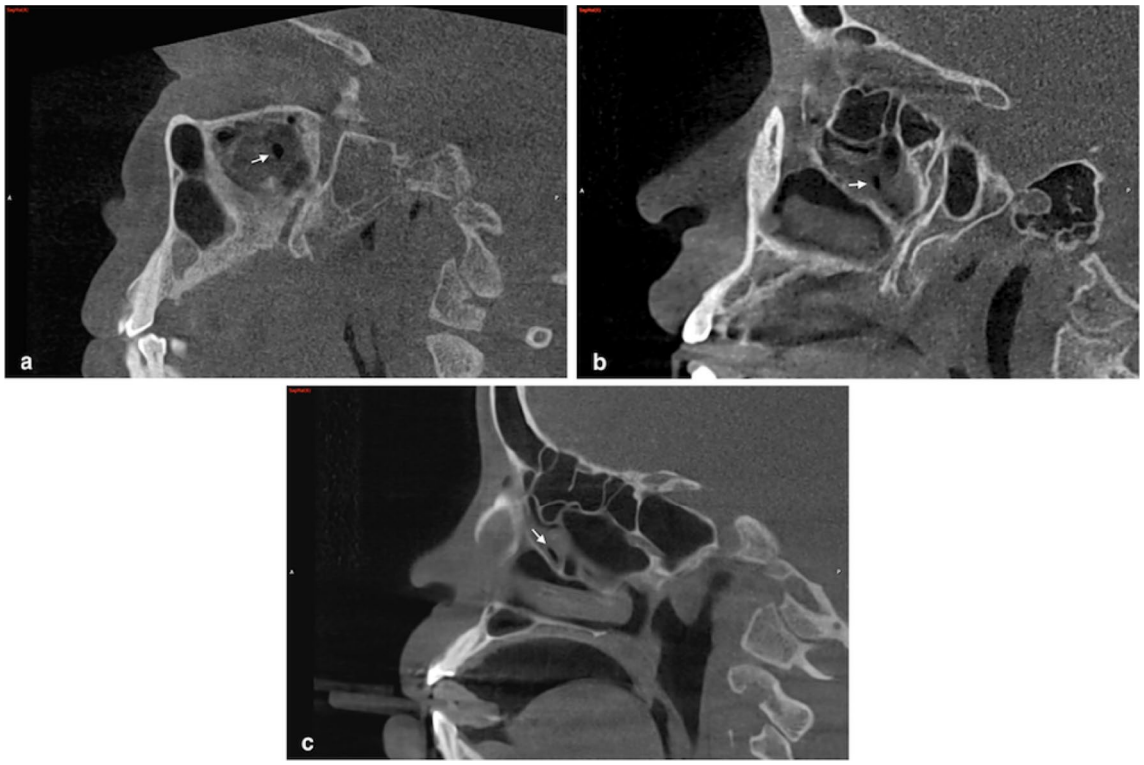

Fig. 3 Representative CBCT images (sagittal views) illustrating the three different shapes of AMOs (white arrow): round (**a**), ovaloid (**b**), and slit shaped (**c**)

Table 4 Potential influencing factors on AMO presence and number

	AMO presence	AMO number (single/multiple)
Patient level		
Age	$p=0.062$[a]	$p=0.613$[a]
Gender	$p=0.740$	$p=0.889$
Sinus level		
Status of the dentition in the posterior maxilla	$p=0.684$	$p=0.679$
Morphological changes of the sinus mucosa	$p=0.828$	$p=0.434$
Endodontic pathology	Healthy 49.6%; Pathological 31.8%; **$p=0.028$***	$p=0.126$
Periodontal pathology	$p=0.124$	$p=1.000$

Chi-square test was performed unless otherwise mentioned

*p value < 0.05 in bold; detailed information such as percentages shown only if significant

[a]Mann–Whitney U test

help to explain that a large AMO reduces nitric oxide concentration and mucus clearance of the respective maxillary sinus, which might make it more susceptible for developing sinus pathology [28]. Therefore, the repair of a large AMOs might be considered to prevent mucous recirculation between the PMO and AMO and maintain the NO reservoir function of the maxillary sinus [19].

On the other hand, the presence of an AMO exhibited a negative association with endodontic pathology in the present investigation. Additionally, having periodontal pathology seems to be a factor associated with a decrease in length of the AMO long axis and AMO surface. These findings might be related to the small number of cases with endodontic and periodontal pathologies included, and the inherent limitation

Table 5 Analysis of the association between the potential influencing factors and the characteristics of the AMOs

	Influencing factor [odds ratio (95% confidence interval), *p* value]					
	Gender (male[a])	Age	Status of the dentition in the posterior maxilla (dentate[a])	Changes of the sinus mucosa (thickening < 2 mm[a])	Endodontic pathology (no pathology/treatment[a])	Periodontal pathology (no pathology[a])
Shape						
Round	0.92 (0.47–1.80), $p=0.801$	0.99 (0.95–1.03), $p=0.754$	2.85 (1.46–5.53), $\mathbf{p=0.002}$	0.73 (0.37–1.43), $p=0.358$	1.52 (0.51–4.53), $p=0.458$	0.99 (0.95–1.03), $p=0.754$
Ovaloid	0.73 (0.38–1.39), $p=0.339$	1.01 (0.97–1.06), $p=0.604$	0.46 (0.24–0.90), $\mathbf{p=0.022}$	1.49 (0.79–2.83), $p=0.216$	0.81 (0.25–2.60), $p=0.719$	1.01 (0.97–1.06), $p=0.604$
Slit shaped	2.58 (0.92–7.24), $p=0.071$	0.99 (0.94–1.04), $p=0.654$	0.55 (0.20–1.53), $p=0.253$	0.79 (0.31–2.02), $p=0.619$	0.55 (0.08–3.77), $p=0.541$	0.78 (0.13–4.57), $p=0.779$
Location						
Within NF/HS	0.92 (0.39–2.18), $p=0.849$	1.04 (0.99–1.09), $p=0.086$	0.72 (0.32–1.66), $p=0.445$	0.90 (0.42–1.96), $p=0.797$	0.40 (0.09–1.73), $p=0.220$	1.17 (0.35–3.88), $p=0.798$
Outside NF and HS	1.09 (0.46–2.57), $p=0.849$	0.96 (0.92–1.01), $p=0.086$	1.38 (0.60–3.17), $p=0.445$	1.11 (0.51–2.41), $p=0.797$	2.49 (0.58–10.68), $p=0.220$	0.86 (0.26–2.84), $p=0.798$
Dimension						
Length of the long axis	1.14 (0.75–1.74), $p=0.547$	0.99 (0.97–1.01), $p=0.134$	0.92 (0.59–1.43), $p=0.702$	1.75 (1.12–2.72), $\mathbf{p=0.013}$	0.89 (0.49–1.61), $p=0.697$	0.56 (0.37–0.85), $\mathbf{p=0.007}$
L/*S* ratio	1.20 (0.99–1.45), $p=0.064$	0.99 (0.99–1.01), $p=0.634$	0.75 (0.61–0.94), $\mathbf{p=0.010}$	0.90 (0.72–1.12), $p=0.349$	0.82 (0.62–1.07), $p=0.137$	1.00 (0.68–1.48), $p=0.995$
AMO area	1.33 (0.35–5.11), $p=0.678$	0.96 (0.91–1.02), $p=0.202$	2.13 (0.44–10.42), $p=0.350$	5.92 (1.32–26.55), $\mathbf{p=0.020}$	1.01 (0.22–4.61), $p=0.989$	0.18 (0.06–0.58), $\mathbf{p=0.004}$

AMO accessory maxillary ostium, *HS* hiatus semilunaris, *NF* nasal fontanelle

p value < 0.05 in bold

[a]Reference category

of CBCT scans using a medium to large FOV and a 0.4 mm voxel size to assess endodontic and periodontal disease. Furthermore, the status of the dentition in the posterior maxilla exhibited a significant association with AMO shape. Partial/complete edentulism was associated with a higher chance of having a round-shaped AMO, while dentate patients were associated with a higher chance of having an ovaloid shape. This result is in line with the finding of a decrease in *L*/*S* ratio associated with partial/complete edentulism compared with a dentate dentition. However, the interpretation of this finding has certainly to be done with great caution due to the lack of a known direct relationship between the status of the dentition and AMO shape. This finding might also result from the interaction of multiple variables, which should be further evaluated by specifically designed studies.

To the best of our knowledge, this is the first study using CBCT images to assess the association of morphological changes of the sinus mucosa, the status of the dentition in the posterior maxilla, and endodontic and periodontal pathology with AMO characteristics. Nevertheless, all findings have to be regarded with some caution, as the present study has several limitations. One of the major limitations is that the CBCT images assessed were retrospectively collected from patients referred for various indications such as implant treatment planning, orthognathic surgery, impacted teeth, cysts, and neoplasias. Furthermore, the included CBCT images were from generally younger patients (mean age 33.3 years), and the number of sinuses associated with endodontic/periodontal pathologies in the posterior maxillary teeth was limited. Therefore, a prospective study specifically recruiting CBCT images from patients with different dentoalveolar pathologies and also including more images from elderly patients would be needed.

Conclusion

In this retrospective study, the AMO frequency in the investigated population was 47.2% (151 sinuses). Only 32 sinuses (21.2%) had more than 1 AMO. Most of the AMOs were located within the region of NF/HS (81.1%) exhibiting a mostly ovaloid (48.4%) or a round shape (39.0%). Pathologies of the maxillary sinus seem to have an impact on AMOs, which was demonstrated by morphological changes of the sinus mucosa being associated with an increase in length and area of AMOs. The exact cause–effect relationship between sinus pathology and AMO dimensions should be further assessed in prospective studies.

Acknowledgements This study was funded by departmental funds only.

Author contributions KFH: data collection, data analysis, manuscript writing. CM: data collection, manuscript editing. AWKY: protocol/project development. GL: manuscript writing and editing. MMB: protocol/project development, manuscript writing and editing.

Funding This study was funded by departmental funds only.

Compliance with ethical standards

Conflict of interest The authors declare that they have no conflict of interest.

References

1. Ali IK, Sansare K, Karjodkar FR, Vanga K, Salve P, Pawar AM (2017) Cone-beam computed tomography analysis of accessory maxillary ostium and Haller cells: prevalence and clinical significance. Imaging Sci Dent 47:33–37
2. Bharathi D, Komala B, Reshma S (2015) Anatomical study of accessory maxillary ostia and its surgical importance. Int J Healthc Sci 2:176–179
3. Bornstein MM, Chappuis V, von Arx T, Buser D (2008) Performance of dental implants after staged sinus floor elevation procedures: 5-year results of a prospective study in partially edentulous patients. Clin Oral Implants Res 19:1034–1043
4. Bornstein MM, Horner K, Jacobs R (2017) Use of cone beam computed tomography in implant dentistry: current concepts, indications and limitations for clinical practice and research. Periodontol 2000 72:51–72
5. Cağlayan F, Tozoğlu U (2012) Incidental findings in the maxillofacial region detected by cone beam CT. Diagn Interv Radiol 18:159–163
6. Capelli M, Gatti P (2016) Radiological study of maxillary sinus using CBCT: relationship between mucosal thickening and common anatomic variants in chronic rhinosinusitis. J Clin Diagn Res 10:MC07–MC10
7. Dedeoglu N, Altun O (2019) Evaluation of maxillary sinus anatomical variations and pathologies in elderly, young, posterior dentate and edentulous patient groups with cone beam computed tomography. Folla Morpholog. https://doi.org/10.5603/FM.a2019.0013
8. Ghosh P, Kumarasekaran P, Sriraman G (2018) Incidence of accessory ostia in patients with chronic maxillary sinusitis. Int J Otorhinolaryngol Head Neck Surg 4:443–447
9. Hoang JK, Eastwood JD, Tebbit CL, Glastonbury CM (2010) Multiplanar sinus CT: a systematic approach to imaging before functional endoscopic sinus surgery. AJR Am J Roentgenol 194:W527–W536
10. Hoang JK, Eastwood JD, Tebbit CL, Glastonbury CM (2010) Multiplanar sinus CT: a systematic approach to imaging before functional endoscopic sinus surgery. Am J Roentgenol 194:W236–W257
11. Hood CM, Schroter RC, Doorly DJ, Blenke EJ, Tolley NS (2009) Computational modeling of flow and gas exchange in models of the human maxillary sinus. J Appl Physiol (1985) 107:1195–1203
12. Hussien A (2013) The association of maxillary accessory ostia with chronic rhinosinusitis what is essential; ventilation or drainage. Life Sci J 10:3958–3966
13. Kumar H, Choudhry R, Kakar S (2001) Accessory maxillary ostia: topography and clinical application. J Anat Soc India 50:3–5
14. Lana JP, Carneiro PM, Machado Vde C, de Souza PE, Manzi FR, Horta MC (2012) Anatomic variations and lesions of the maxillary sinus detected in cone beam computed tomography for dental implants. Clin Oral Implants Res 23:1398–1403
15. Mahajan A, Mahajan A, Gupta K, Verma P, Lalit M (2017) Anatomical variations of accessory maxillary sinus ostium: an endoscopic study. Int J Anat Res 5:3485–3490
16. Mancl LA, Leroux BG, DeRouen TA (2000) Between-subject and within-subject statistical information in dental research. J Dent Res 79:1778–1781
17. Mladina R, Skitarelić N, Casale M (2010) Two holes syndrome (THS) is present in more than half of the postnasal drip patients? Acta Otolaryngol 130:1274–1277
18. Ozel HE, Ozdogan F, Esen E, Genc MG, Genc S, Selcuk A (2015) The association between septal deviation and the presence of a maxillary accessory ostium. Int Forum Allergy Rhinol 5:1177–1180
19. Penttilä M (2018) Accessory maxillary ostium repair using middle turbinate flap: a case series of 116 patients with chronic rhinosinusitis. Int Forum Allergy Rhinol 8:1204–1210
20. Prasanna LC, Mamatha H (2010) The location of maxillary sinus ostium and its clinical application. Indian J Otolaryngol Head Neck Surg 62:335–337
21. Rice HD, Scheaffer SD (1993) Endoscopic paranasal sinus surgery. Raven Press, New York
22. Sahin C, Ozcan M, Unal A (2015) Relationship between development of accessory maxillary sinus and chronic sinusitis. Med J DY Patil Univ 8:606–608
23. Singhal M, Singhal D (2014) Anatomy of accessory maxillary sinus ostium with clinical application. Int J Med Sci Public Heal 3:327–329
24. Soikkonen K, Ainamo A (1995) Radiographic maxillary sinus findings in the elderly. Oral Surg Oral Med Oral Pathol Oral Radiol Endod 80:487–491
25. Souza AD, Rajagopal KV, Ankolekar VH, Souza AD, Kotian SR (2016) Anatomy of maxillary sinus and its ostium: a radiological study using computed tomography. CHRISMED J Health Res 3:37–40
26. Timmenga NM, Raghoebar GM, Liem RS, van Weissenbruch R, Manson WL, Vissink A (2003) Effects of maxillary sinus floor elevation surgery on maxillary sinus physiology. Eur J Oral Sci 111:189–197
27. Vogiatzi T, Kloukos D, Scarfe WC, Bornstein MM (2014) Incidence of anatomical variations and disease of the maxillary sinuses as identified by cone beam computed tomography: a systematic review. Int J Oral Maxillofac Implants 29:1301–1314
28. Yenigun A, Fazliogullari Z, Gun C, Uysal II, Nayman A, Karabulut AK (2016) The effect of the presence of the accessory maxillary ostium on the maxillary sinus. Eur Arch Otorhinolaryngol 273:4315–4319
29. Yeung AWK, Colsoul N, Montalvao C, Hung K, Jacobs R, Bornstein MM (2019) Visibility, location, and morphology of the primary maxillary sinus ostium and presence of accessory ostia: a retrospective analysis using cone beam computed tomography (CBCT). Clin Oral Investig. https://doi.org/10.1007/s00784019028299